IJCSI International Journal of Computer Science Issues, Volume 17, Issue 3, May 2020
ISSN (Print): 1694-0814 | ISSN (Online): 1694-0784
www.IJCSI.org https://doi.org/10.5281/zenodo.3987147

The Frequency Distributions and Variability of Threshold Voltage Induced by NBTI and HCI Degradations in Si Nanowire FETs

Abderrezak Bekaddour, Marco G. Pala, Nasr-Eddine CHABANE SARI and Gérard Ghibaudo

***Abstract*—we present a strong methods of two studies that were reviewed, which demonstrated a well bounded case of the trap-charge-induced variability of threshold voltage in silicon-nanowire FETs. By using full-quantum 3-D simulations, we proof and analyse the transfet characteristics in the attendance of discrete trap charges at different positions in the gate-stack volume, and we calculate the probability density function of these 3D randomly distributed impurities. Entertaining a Poisson distribution for the trap charge numbers, we compute approximation of the statistics of the threshold voltage shift induced by such charged defects and evaluate the mean value, the standard deviation, the skewness and the kurtosis of the threshold voltage for typical trap density values.**

***Index Terms*—Nonequilibrium Green's functions (NEGF) method, remote Coulomb scattering (RCS), Negative Bias Temperature Instability (NBTI), Hot Carrier Injection (HCI), GAA silicon-nanowire (Si NW) transitors (GAA-SNWTs), variability.**

I. INTRODUCTION

AS the channel lenghts of prevailing planar metal-oxide-semiconductor field effect transistors (MOSFETs) condense into the nanometer scale, the device fulfilment is debased by short-channel effects emergent from the weakened gate control. To crack this problem, strongly confined multigate transistors as gate-all-around (GAA) silicon nanowire (Si NW) FETs have been suggested as promising devices to accomplish the conditions of the technological roadmap of semiconductors [1] .

Nanowire MOSFETs have been the major force behind the potential development in the nano-electronics industry, to bring in without precedent scientific and technological improvement. This essential impact of nano wire MOSFETs has been managed by the phenomenal properties of both Si and its oxide SiO_2 or better the High-κ . The progress in nanowire MOSFET based nano-electronics has not been without its problems. The functioning requirements of ICs put stress on the devices, leading to performance and reliability problems. NW MOSFETs, and especially the oxide and high-κ, degrade during the device operation and cannot retain its original specifications.

A. Bekaddour is with U.R.M.E.R University of Abou Bekr Belkaid Tlemcen, BP 119, 13000 Tlemcen Algeria
M. G. Pala is with Centre de Nanosciences et de Nanotechnologies CNRS, Universit Paris-Sud, Universit Paris-Saclay 10 Boulevard Thomas Gobert -91120 Palaiseau, France
N.-E. CHABANE SARI is with U.R.M.E.R University of Abou Bekr Belkaid Tlemcen, BP 119, 13000 Tlemcen Algeria
G. Ghibaudo is with IMEP-LAHC (UMR CNRS/INPG/UJF 5130), Grenoble INP Minatec, 3 Parvis Louis Néel, BP 257, F-38016 Grenoble, France

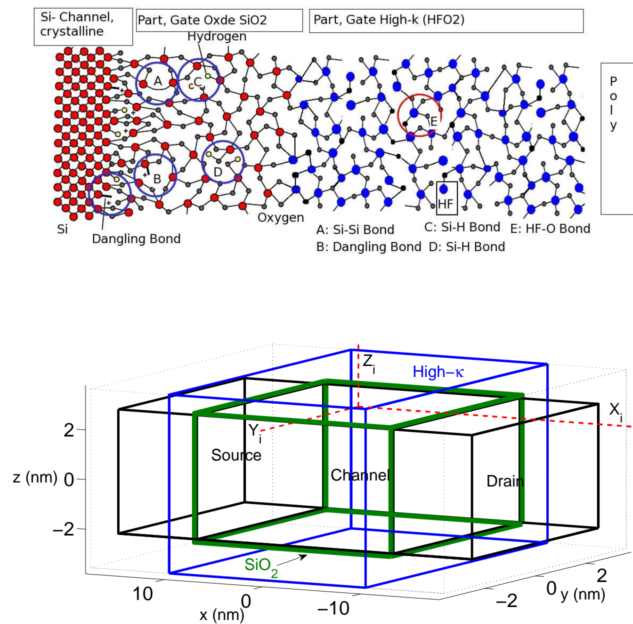

Fig. 1. (Top) Si, Si/SiO_2 interface, SiO_2/high-κ interface, high-κ, and oxide/high-κ defect structure and dangling Si bonds are shown. (bottom) Schematic view of the GAA Si-NW FET consisting of a 20-nm undoped channel and 10-nm S/D regions nominally doped at $10^{20}\mathrm{cm}^{-3}$. The cross section of the devices is $5 \times 5\mathrm{nm}^2$, and the SiO_2 oxide and High-κ thickness are 0.2-nm, 0.8-nm respectively.

However, the degradation type is defect generation in the oxide/high-κ or at the Si-SiO_2 interface over time. The defects can increase easily the leakage current through the gate dielectric, change transistor metrics such as the threshold voltage or result in the device failure due to oxide breakdown.

Negative Bias Temperature Instability (NBTI) is one of the most important threats to NMOSFETs in VLSI circuits. The electrical stress on the transistor generates traps at the Si-SiO_2-high-κ. These defect sites increase the threshold voltage, reduce channel mobility of the NW MOSFETs or induce parasitic capacitances and degrade the performance. Hot Carrier Injection (HCI), although alleviated for current generation NW MOSFETs, is another mechanism that can generate defects at the Si-SiO_2 interface near the drain (less near the source) edge

IJCSI
www.IJCSI.org

as well as in the oxide bulk.
However, lot off works published, treating the NBTI experimentally on PMOSFET and especially with high temperature [3] .In parallel, few works talking on atomistics study of NBTI [4]. Modeling and simulation [6], In conventional Si MOSFETs, the transistors are annealed in hydrogen ambient to passivate the dangling Si bonds during manufacture [2]

NBTI has gained tremendous scientific and industrial interest as it can lead to severe shifts of important transistor parameters, as the threshold voltage or the drain current, and seems to be accelerated in recent technologies which rely on nitrided oxides, high-k dielectrics, and other novel approaches. The exact physical background is still not completely understood but the general consensus is that the Si/SiO2 interface is damaged and interface traps and/or interface charges and probably oxide charges cause the degradation. For the modeling of NBTI the carrier concentration close to the Si/SiO2/high-k interfaces plays an important role. The classical simulation using the drift-diffusion approximation gives the highest magnitude of the electron concentration at the Si/SiO2 interfaces below the gate contacts. It can be seen that the peak electron concentration is found in the top corners, as two respective gates couple to the channel, each of them attracting carriers. With the quantum confinement correction models the maximum carrier concentration is moved to the inside of the fin by a distance depending on the chosen model and its calibration parameters. The use of quantum confinement models reduces this carrier concentration and might have significant influence on the NBTI model used. In classical device simulators quantum confinement is often accounted for by using additional quantum correction models. These models locally change the carrier density-of-states [10, 11] or they modify the conduction band edge close to the interface [12].

In this work, NBTI and HCI degradation and their implications on NW device reliability are studied. First, part 2 presents the NBTI, HCI background and the theory for NBTI, HCI degradation from the perspective of Reaction-Diffusion phenomenon . Physical models are presented in section III . The impact of NBTI, HCI degradation on GAA NW MOSFET characteristics is investigated in section IV. Future directions are provided and conclusions in section V.

II. Physical Mechanisms of NBTI and HCI degradation

Before talking about defaults-charges interactions, we will discus clearly the original of defaults and the structure of metallic oxyde hifg-k. The structure of metallic oxyde such as HfO2 is certainly less stiff than SiO2. That meaning, its d orbital electrons strongly delocalized of ion metallic bonds [5]. However, in Fig 1 (Top) the electrons of bonds are very sensitive of positions and chemical atomics bonds Oxygen and hers neighbours metallic ions; so much atoms in structure considered. NBTI and HCI degradation are a significant reliability concern for nanoscale CMOS circuits which manifests itself as an increase in thershold voltage that reduces switching speed. At the atomic level, NBTI is caused by an electric field dependent disassociation of Si-H bonds at the Si-SiO2 interface. In general, the crystallization of high-k wouldn't wish; because is causes ununiformity of Oxyde distribution. Among the disadvantages of high-k polycristallinity have been the ion diffusion is many order acceleration in interfaces. In contrast, the structure rigidity of the metal oxides also prevents an easy healing defects after annealing since it requires a significant rearrangement of the closest neighboring atoms. The freed hydrogen diffuses into the oxide, resulting in interface traps that increases the threshold voltage. This disassociation is most prevalent for PMOSFETs under negative bias (Vgs = -Vdd) [16, 17, 18]. When the stress is removed (Vgs = 0), the diffusions reverses and some of the hydrogen can rebond with the Si, removing the interface traps [19, 20, 21]. This reversal is called the recovery effect. Deficiencies of Oxygens, with an energy level near to the conduction band of silicon [5], would be responsible for a trapping electrons injected from the transistor channel. This leads to unstability of the threshold voltage of MOSFET device and finally reduces the inversion charge and also the reduction of drain current, that proofed by [6],[7]. It also appears clear that a trapping; greatly decreases when using HfSiO or HfSiON [7] A study was developed of Hafnium Silicates demonstrating a reduction of mobility at low field (Coulomb interaction) when the concentration of HF and the density of crystallization area are increase, and keeping the same sense [8]. Furthermore, the phase separation in silicates leads to no-uniformity of the dielectric film composition, which may be associated the variations in the oxide capacitor COX-eff along the channel [8]. This fluctuation of capacity, acting locally on the value of effective field, degradation of carrier mobility in strong filed and would be similar the roughness surface interaction mechanism [9]

III. Physical models

Numerical simulations are performed by self-consistently solving the 3-D Schrödinger and Poisson equations in the coherent transport regime in the presence of fixed charge centers trapped at the SiO_2/high-κ dielectric interface.

In order to reduce the numerical burden the coupled mode space (CMS) approach is used within the NEGF formalism [22]. According to the CMS approach the discrete electron correlation function reads:

$$G^{<}(i_1,i_2,j_1,j_2,k_1,k_2;E) = \sum_{n,m} G^{<}_{\mathrm{ms}}(i_1,i_2,n,m;E)\phi^{n}_{i_1}(j_1,k_1)\phi^{m*}_{i_2}(j_2,k_2)\ , \quad (1)$$

where $\{\phi^n_i\}_{n=1,2,\ldots,N_yN_z}$ is the orthonormal set of eigenfunctions solution of the 2-D Schrödinger problem for the ith slice of the device, $G^{<}_{\mathrm{ms}}$ is the mode-space counter part of the real-space Green's function and $N_y(N_z)$ indicates the number of discretization nodes along the $y(z)$ confinement direction. The solution in the transverse plane is obtained assuming close boundary conditions with vanishing wave functions at the gate-oxide interface. The Green's functions in the mode space are

IJCSI International Journal of Computer Science Issues, Volume 17, Issue 3, May 2020
ISSN (Print): 1694-0814 | ISSN (Online): 1694-0784
www.IJCSI.org https://doi.org/10.5281/zenodo.3987147

obtained as solution of the two of kinetic equations

$$[E - H_{\rm ms} - \Sigma_{\rm ms}]\, G_{\rm ms} = I \qquad (2)$$
$$G^{<}_{\rm ms} = G_{\rm ms}\Sigma^{<}_{\rm ms}G^{\dagger}_{\rm ms},$$

where $\Sigma^{<}_{\rm ms}$ and $\Sigma_{\rm ms}$ are the lesser-than and retarded self-energies describing the ideal infinite equipotential contacts, $H_{\rm ms}$ is the mode-space Hamiltonian and I is the identity matrix, for every energy E, and then evaluating the real space electron density through the integral:

$$n_{i,j,k} = \frac{-ig_v g_s}{\Delta x} \int \frac{\mathrm{d}E}{2\pi} G^{<}(i,i,j,j,k,k;E) \;, \qquad (3)$$

where $g_{v,s}$ are the valley and spin degeneration coefficients, respectively.

The Poisson equation

$$-\nabla \cdot (\epsilon(\mathbf{r})\nabla\phi(\mathbf{r})) = \rho(\mathbf{r}) \qquad (4)$$

is solved in the 3-D domain using the box-integration method, where $\epsilon(\mathbf{r})$ is the position dependent dielectric constant, $\rho(\mathbf{r})$ is total charge density accounting for both electrons and fixed charges, and $\phi(\mathbf{r})$ is the self-consistent electrostatic potential.

IV. Methodology and results

For the evaluation of the quantum study models a state-of-the-art three-dimensional N- channel GAA device structure was chosen. The device geometry can be seen in Fig.1 (bottom). We consider, the silicon [100] fin has a cross section area of 5×5 nm^2 and gate length of 20 nm.. The source and drain regions are heavily n-type doped whereas the channel itself remains undoped. The S/D regions are 10 nm long with a donor-doping concentration of $N_D = 10^{20}$ cm^{-3}. An interfacial layer of silicon oxide with thikness $t_{\rm IL} = 0.2$ nm is placed between the silicon channel and the high-k gate dielectric (HfO_2). The dielectric propreties of the high-k and of SiO_2 interfacial layer are assumed thikness independant. Discrete charged defects can be located inside the gate-stack volume at position (x_i, y_i, z_i) and the Si/SiO_2 interfaces. Applied source-drain voltage is V_{DS} =10mV, and the temperature is $T = 300$ K. The tansfer characteristics of such devices in the presence of a single trap carge located at the Si/SiO_2/ high-κ interfaces and at different positions along the $x - y - z$ volume are shown in Fig. 2, where the on- turn curve of a clean device is plotted as the reference. We notice a systematic positive threshold voltage shift due to the additional barrier on the device subbands induced by the negatively charged defect. The current amplitude variation $\Delta I_D = I_D - I^{\rm ball}_D$ induced by this additional barrier can be associated to the NBTI , HCI degradation. It presnts an almost constant value in the subthreshold voltage regime and then strongly decreases for positive gate overdrive values due to electrostatic screening.

This behavior of the NBTI and HCI amplitude with gate voltage can reasonably be related to the transistor gain according to the analytical formula proposed in Ref. [23] , [13, 14, 15]:

$$\frac{\Delta I_D}{I_D} = -\frac{g_m}{I_D}\frac{q}{C_{\rm ox}}\left(1 - \frac{z_t}{t_{ins}}\right), \qquad (5)$$

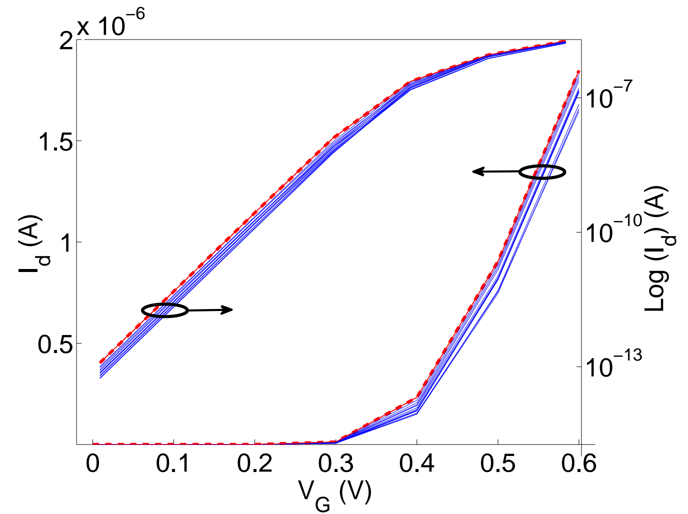

Fig. 2. (Solid blue lines) $I_d - V_G$ characteristics of the GAA nanowire Si-MOSFET with the single charge trapping $M_i = (x_i, y_i, z_i)$ inside of channel. (Dashed red line) The smooth device is also shown for comparison.

where g_m the transconductance and $C_{\rm ox}$ the total gate capacitance and z_t the trap depth in the dielectric of thickness t_{ins}.

A nice agreement between the analytical model and the numerical calculation is proofed in Ref. [2]. The dependence of the threshold voltage shift on the position along the three spacial directions of the single charged impurity is studied, such that; we defined (ΔV_T here at constant current $I_D(A) = 10^{-12}, 10^{-11}, 10^{-9}, 10^{-7}, 5.010^{-7}$ and 10^{-6}, corresponding the interval of $V_G(V) \in [0,\ 0.1], [0.1,\ 0.2], [0.2,\ 0.3], [0.3,\ 0.4], [0.4,\ 0.5], [0.5,\ 0.6]$ respectively. By fastening the trap-charge defect at the interface, it was possible to systematically study the influence of the position on the volume (x,y,z) of the trap on the VT variability and to generate by 3-D extrapolation the threshold voltage variation map. However, at low VG and inferior of device threshold voltage Vth, we found a stronger decrease of parabolic forms Delta VT as far as the impurity is moved away from the interface along the vertical direction and drenching in depth of dielectric shown in top of Fig.5 . This behavior is primarily due to the usual remote coulomb scattering effect depicted in (5) and additionally due to the different permittivities present in the SiO_2 layer and the high-k dielectric in the gat stack as well as for the wive-function penetration inside the dielectric. On the other hand, at strong VG and superior of device threshold voltage Vth, we shown in bottom of fig.5, that the parabolic forms divided in two half no symmetrically parabolic forms converging to Drain and Source, when VG increasing. Note that, as drain voltage is nicely have an influence, so the corner effect is shown clearly (as rotation phenomenon) near of borders.

V. Variability and statistical study of NBTI, HCI degradation

From 3D-maps shown in figure 3 and by exploiting these data, we estimated the statistical properties of a single charge trap randomly distributed in the volume. Here, this is achieved by generating 8 120 601 (201 x 201 x 201) random positions

IJCSI
www.IJCSI.org

IJCSI International Journal of Computer Science Issues, Volume 17, Issue 3, May 2020
ISSN (Print): 1694-0814 | ISSN (Online): 1694-0784
www.IJCSI.org https://doi.org/10.5281/zenodo.3987147

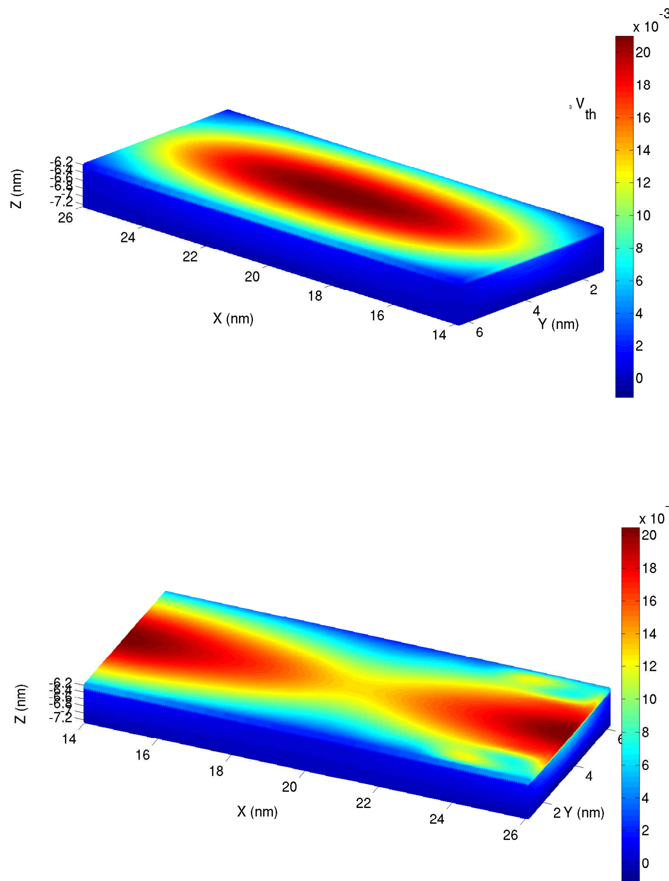

Fig. 3. Maps of threshold voltage shift as a function of the position of a single trap charge drenching in the depth of dielectric along the volume $x-y-z$ at (Top) $V_G(V) \in [0.0,\ 0.1]$ and (bottom) $V_G(V) \in [0.4,\ 0.5]$

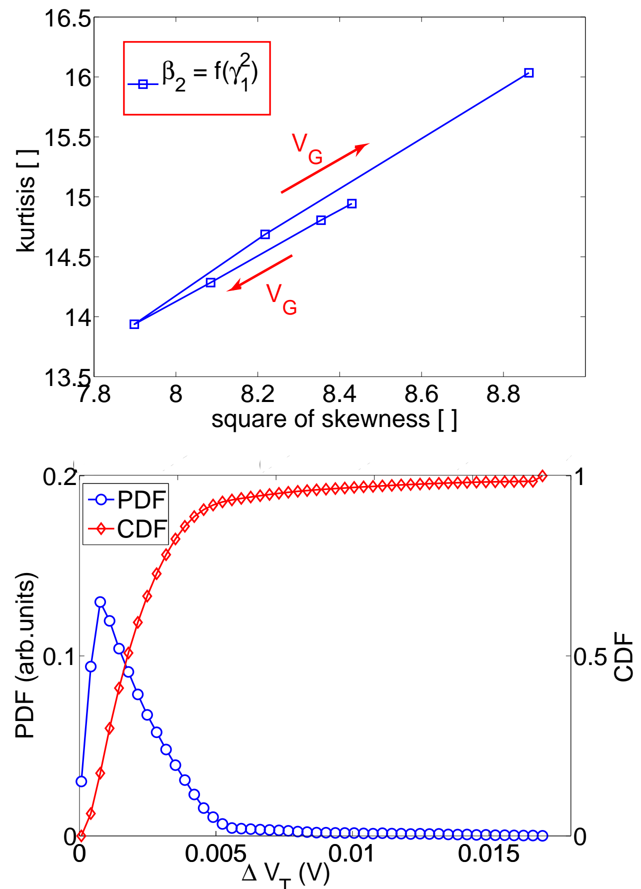

Fig. 4. (Top) Kurtosis of joined-half-Gaussian distribution versus square of skewness, such that $V_G(V) \in [0.0,\ 0.6]$. (bottom) Probability density function (circle line points) and the corresponding cumulative distribution function (diamond line points) of having a determined value of ΔV_T due to a single discrete trap charge in the Si/SiO2/high-κ interfaces at $V_G \in$ [0.3,0.4].

uniformly distributed on the volume for each VG value and hence by calculating the corresponding PDF and its CDF shown in Fig 4 (bottom) (we restrict only for VG= 0.4 curve). In order to obtain an almost continuous curve, a discretization step delta Delta VT = 0.4 mv has been considered. Such a deterministic approach has the advantage to be expensive than a statistical treatment consisting in computing a complete set of simulation for a given set of random positions. On the other hand, as the frequency function for a Gaussian distribution reads:

$$f\left(\Delta V_T\right)=\frac{1}{\sqrt{2\pi}\sigma_p}.\exp\left(-\frac{\left(\Delta V_T-\mu_p\right)^2}{2\sigma_p^2}\right), \qquad (6)$$

A Gaussian distribution has a skewness = 0 and a kurtosis = 3. The approximation of a true profile with a Gaussian distribution is only accurate to first order. However, the simplicity of the calculation justifies to some degree its use when the primary concern is the average location and average extent of a distribution. When we went to fit more accurately the asymmetrical distribution usually found in practice, it is necessary to at least account for the skewness. The frequency function is defined to consist of two half Gaussian distributions that join at a modal projected range Rm. When $\Delta V_T < Rm$, the distribution has standard deviation σ_1; while for $\Delta V_T > R_m$, the distribution has standard deviation σ_2. The formulation $f\left(\Delta V_T\right)$ becam:

$$\begin{cases} \frac{1}{\sqrt{2\pi}(\sigma_1+\sigma_2)}.\exp\left(-\frac{(\Delta V_T-\mu_m)^2}{2\sigma_1^2}\right) & \Delta V_T < \mu_m \\ \frac{1}{\sqrt{2\pi}(\sigma_1+\sigma_2)}.\exp\left(-\frac{(\Delta V_T-\mu_m)^2}{2\sigma_2^2}\right) & \Delta V_T > \mu_m \end{cases} \qquad (7)$$

The modal projected range μ_m, σ_1 and σ_2 can be calculated by using the characteristic quantities (conventional formulation probability) as shows in Fig 4 (Top). With some amount of algebra these integrals evaluate to:

$$\mu_p=\mu_m+\sqrt{\frac{2}{\pi}}(\sigma_2-\sigma_1) \qquad (8)$$

$$\sigma_p=\sqrt{(\sigma_1^2-\sigma_1.\sigma_2+\sigma_2^2)-\frac{2}{\pi}(\sigma_2-\sigma_1)^2} \qquad (9)$$

$$\gamma_p=\frac{\sqrt{\frac{2}{\pi}}(\sigma_2-\sigma_1)\left((\frac{4}{\pi}-1)(\sigma_1^2+\sigma_2^2)-(3-\frac{8}{\pi})\sigma_1.\sigma_2\right)}{\sigma_p^3} \qquad (10)$$

We found from our simulation and for different V_G, the following table Tab1, and to evaluating all parameter μ_m,

IJCSI International Journal of Computer Science Issues, Volume 17, Issue 3, May 2020
ISSN (Print): 1694-0814 | ISSN (Online): 1694-0784
www.IJCSI.org https://doi.org/10.5281/zenodo.3987147

$V_G \in$	$R_p[mV]$	$\sigma_p[mV]$	$\gamma_p[]$	$\beta_p[]$
[0.0, 0.1]	2, 5988	2, 4781	2, 9034	14, 9436
[0.1, 0.2]	2, 6331	2, 4949	2, 8904	14, 8050
[0.2, 0.3]	2, 7275	2.5309	2.8434	14, 2847
[0.3, 0.4]	2, 2611	2.0791	2, 8104	13, 9372
[0.4, 0.5]	2, 4136	2, 2911	2, 8667	14, 6867
[0.5, 0.6]	2.6459	2, 6444	2, 9769	16, 0346

TABLE I
NUMERICAL VALUES FOR PROJECTED RANGE, THE STANDARD DEVIATION, THE SKEWNESS AND THE KURTOSIS OF TOW HALF GAUSSIAN DISTRIBUTIONS OF DIFFERENT VALUES OF V_G.

σ_1, σ_2; we suggest to using an iterative methods (Newton methods,...).
Moreover, we notice that such an approach can be easily extend to charged traps localized on specific spacial regions as grain-boundary lines of high-κ materials. This is particularly beneficial for $3-D$ NEGF quantum simulations which are very much time consuming. In order to evaluate the variability induced by discrete trap charges in the oxide/high-κ of small devices, we have to consider that the number of these impurities is statistically distributed according to a Poisson law with the mean value determined by the nominal trap density N_t.

We verified that the addition of two or more trap charges in the oxide/high-κ is almost independent of each other and that it gives rise to an overall ΔV_T cumulating the single-charge contributions.

Therefore, we assume that, for each device, the global ΔV_T shift, $\Delta V_{T,\mathrm{tot}}$, is given by

$$\Delta V^j_{T,\mathrm{tot}} = \sum_{j=1}^{N^j_{t,\mathrm{tot}}} \Delta V_{T,i} \tag{11}$$

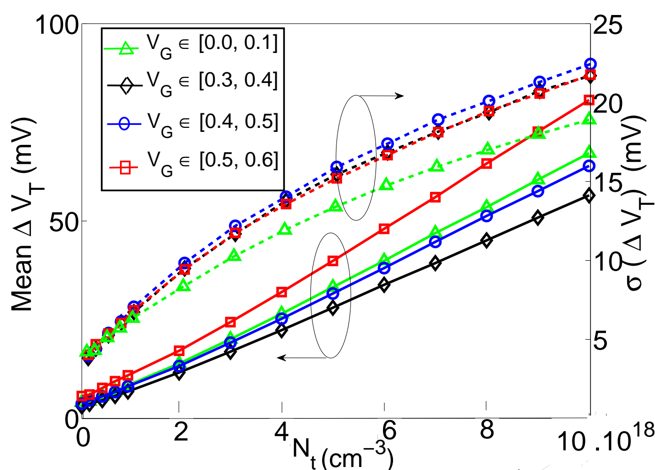

Fig. 5. Mean value and standard deviation of the threshold voltage shift probability due to the NBTI and HCI degradations density N_t.

where $\Delta V_{T,i}$ is the contribution of the ith trap and $N^j_{t,\mathrm{tot}}$ is the number of trap charges in the jth simulated device. The number of traps $N^j_{t,\mathrm{tot}}$ is randomly generated from a Poisson law having a mean value $N_t V$, V being the volume of the

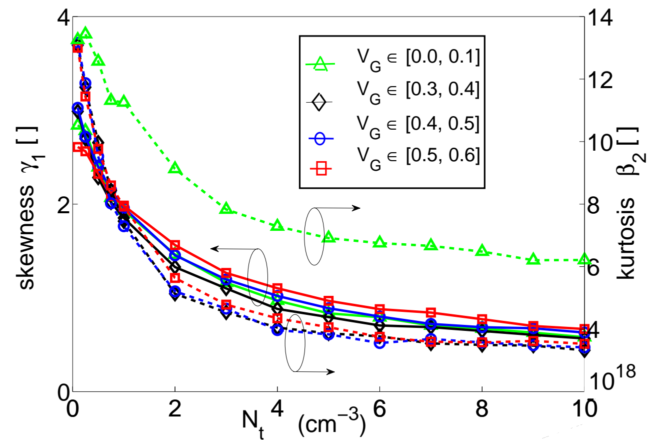

Fig. 6. The kurtosis and the skewness of the threshold voltage shift probability due to the NBTI and HCI degradations density N_t.

device active volume (here $V = 536.8$ nm^3). The $\Delta V_{T,i}$ are randomly generated using the PDF of the elementary charge ΔV_T distribution of Fig. 4. and for different V_G value intervals. By this methode, we could obtain, as shown in Fig.5 and Fig.6, the evolution with the average trap charge density Nt of the first four statistical mements of the Delta VT probability distribution. The behavior of the mean value (smooth lines) for different VG, of the standard deviation (dashed line) also for different VG, of the skewness (lines) and of the kurtosis (lines) at the large value of Nt is determined by the Poissonian distribution of the number of interface trap charges. In particular, we observe in Fig.7 an almost linear increase of the mean threshold voltage shift, a power-law increase of the standard deviation, and a clear decrease of the skewness and kurtosis with Nt. Finally, of course, the simulation of the present paper to have an influence on the industrial of fabrication but more on the characterization (even as a nano-bio-sensor) of NW-MOSFET; this is why the important part of this work that, the statistical characteristic quantities can either be calculated or measured in order to fit an assumed frequency function to experimentally determined trapping charges profiles Nt. However, we propose the easiest approach for that task is a simple polynomial fit:

$$Mean(\Delta V_T) = \sum_{i=0}^{n} a_i.N_t^i \tag{12}$$

$$\sigma = \sum_{i=0}^{n} b_i.N_t^i \tag{13}$$

$$\gamma = \sum_{i=0}^{n} c_i.N_t^i \tag{14}$$

just find the inverse problem; the coefficients for such polynomials are given in Table 2, Table 3 and Table 4 respectively for different values of V_G. The dimension of the coefficients a_i, b_i are $mV peri-th$ power of the units used for trapping, usually cm^{-3} in the range $[10^{17}, 10^{19}]$. The skewness γ has not been approximated in this way, although there in principal

$V_G(V) \in$	$[0.0,\ 0.1]$	$[0.1,\ 0.2]$	$[0.2,\ 0.3]$	$[0.3,\ 0.4]$	$[0.4,\ 0.5]$	$[0.5,\ 0.6]$
a_0	$3,468$	3.500	3.421	$2,696$	$3,338$	4.921
a_1	$4.266.10^{-18}$	$4,032.10^{-18}$	$4,403.10^{-18}$	$3,608.10^{-18}$	$4,301.10^{-18}$	$5.467.10^{-18}$
a_2	$5,908.10^{-37}$	$8,214.10^{-37}$	$5,238.10^{-37}$	$5,500.10^{-37}$	$3,897.10^{-37}$	$3,911.10^{-37}$
a_3	$-6,839.10^{-56}$	$-1,323.10^{-55}$	$-3.514.10^{-56}$	$-7,172.10^{-56}$	$-2,507.10^{-56}$	$-1,536.10^{-56}$
a_4	$3,974.10^{-75}$	$1,105.10^{-74}$	$-1,288.10^{-75}$	$4,607.10^{-75}$	$1,723.10^{-76}$	$-5,938.10^{-76}$
a_5	$-9,371.10^{-95}$	$-3,663.10^{-94}$	$1,643.10^{-94}$	$-1,161.10^{-94}$	$1,981.10^{-95}$	$3,243.10^{-95}$

TABLE II
COEFFICIENTS FOR $R_p\ (mV)$ ON DIFFERENT INTERVALES OF V_G.

$V_G(V) \in$	$[0.0,\ 0.1]$	$[0.1,\ 0.2]$	$[0.2,\ 0.3]$	$[0.3,\ 0.4]$	$[0.4,\ 0.5]$	$[0.5,\ 0.6]$
b_0	$3,765$	$3,689$	3.482	$2,804$	$3,650$	5.759
b_1	$3,560.10^{-18}$	$3,569.10^{-18}$	$3,657.10^{-18}$	$3.069.10^{-18}$	$3,552.10^{-18}$	$4,867.10^{-18}$
b_2	$-3.605.10^{-37}$	$-2,866.10^{-37}$	$-3,506.10^{-37}$	$-3,234.10^{-37}$	$-3,941.10^{-37}$	$-5,740.10^{-37}$
b_3	$3,434.10^{-56}$	$8,360.10^{-57}$	$1,903.10^{-56}$	$2,638.10^{-56}$	$4,092.10^{-56}$	$7,237.10^{-56}$
b_4	$-2,337.10^{-75}$	$9,536.10^{-76}$	$3,103.10^{-76}$	$-1,119.10^{-75}$	$-2,721.10^{-75}$	$-6,113.10^{-75}$
b_5	$7,733.10^{-95}$	$-6,352.10^{-95}$	$-5,322.10^{-95}$	$1,647.10^{-95}$	$8.288.10^{-95}$	$2,272.10^{-94}$

TABLE III
COEFFICIENTS FOR $\sigma_p\ (mV)$ ON DIFFERENT INTERVALES OF V_G.

$V_G(V) \in$	$[0.0,\ 0.1]$	$[0.1,\ 0.2]$	$[0.2,\ 0.3]$	$[0.3,\ 0.4]$	$[0.4,\ 0.5]$	$[0.5,\ 0.6]$
c_0	3219.153	3078.336	$3046,943$	$3021,693$	$3165,843$	$2968,339$
c_1	$-1,932.10^{-15}$	$-1,584.10^{-15}$	$-1.675.10^{-15}$	$-1,588.10^{-15}$	$-1,742.10^{-15}$	$-1,502.10^{-15}$
c_2	$7,255.10^{-34}$	$5,201.10^{-34}$	$5,904.10^{-34}$	$5,132.10^{-34}$	$6,249.10^{-34}$	$5,502.10^{-34}$
c_3	$-1,388.10^{-52}$	$-9.107.10^{-53}$	$-1,097.10^{-52}$	$-8,759.10^{-53}$	$-1,168.10^{-52}$	$-1,064.10^{-52}$
c_4	$1,266.10^{-71}$	$7,850.10^{-72}$	$9,895.10^{-72}$	$7,354.10^{-72}$	$1,050.10^{-71}$	$9,837.10^{-72}$
c_5	$-4,361.10^{-91}$	$-2,609.10^{-91}$	$-3,402.10^{-91}$	$-2,384.10^{-91}$	$-3,586.10^{-91}$	$-3,429.10^{-91}$

TABLE IV
COEFFICIENTS FOR γ_1 ON DIFFERENT INTERVALES OF V_G.

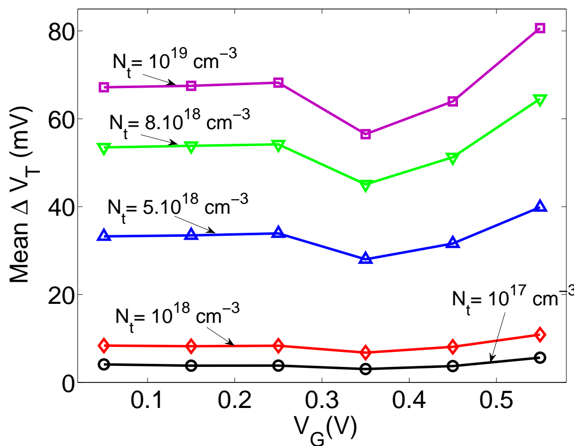

Fig. 7. The mean of threshold voltage ΔV_T versus gate voltage V_G of having a determined value of due to a given NBTI and HCI degradations density N_t .

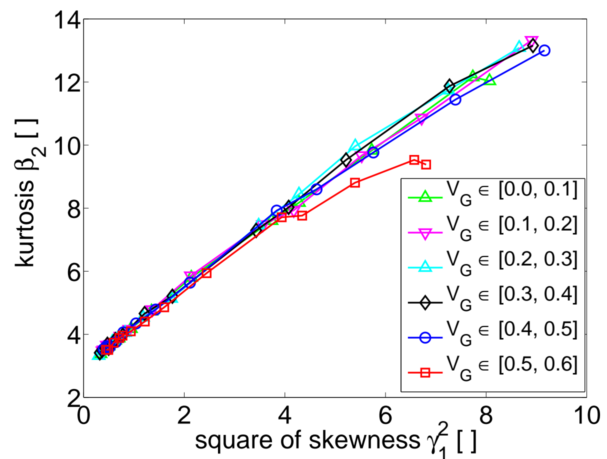

Fig. 8. Kurtosis of Poissonian distribution versus square of skewness.

no problem, but for construction of distributions for which an accurate value of the skewness is required as shows in Fig.8.

VI. CONCLUSION

In conclusion, we have studied the variability of threshold voltages induced by discrete trap charges present in negative bias temperature instability and hot carrier injection of GAA Si-NWFETs. By performing 3-D self-consistent simulations within the NEGF formalism, we have first evaluated the effect on the transfet characteristics of a single trap charge located inside the insulator. Hence, we have presented a semianalytical method exploiting the probability function due to such asingle trap charge to obtain the PDF due to a Poissonian number of discrete traps. Our results indicate a significant V_T variation in case of N_t larger then $10^{18}\ cm^{-3}$, mainly resulting from

the Poisson-distributed number of traps.

Finally, we remark that such a methodology could be applied to simulate the variability of other kinds of discrete defects as, for example, traps, dopants, or other localized impureties in short-channel devices, with the advantage of a huge gain in computationl time.

Competing financial interests

The authors declare no competing financial interests.

References

[1] ITRS Roadmap 2009, available at *www.itrs.net/Links/2009ITRS*.

[2] A.Bekaddour, M.Pala, N.E Chabansari, G. Ghibaudo, "Deterministic method to evaluate the threshold voltage variability induced by discrete trap charges in Si-Nanowire FETs" *IEEE Trans. Electron Devices*, 59, no.5, p.1462- 1467, 2012 .

[3] B. Djezzar, H. Tahi, A. Benabdelmoumene, A. Chenouf, "A propagation concept of negative bias temperature instability along the channel length in p-type metal oxide field effect transistor " *Solid-State Electronics*, 82 p4653, 2013.

[4] E. Lee and H.Ju, Journal of the Korean Physical Society, Vol. 52, No. 2, February 2008, pp. 337-341 "Mechanism for Nitrogen-Originated Negative-Bias Temperature Instability in a MOSFET with a Si-Oxynitride Gate Dielectric" Journal of the Korean Physical Society, Vol. 52, No. 2, February 2008, pp. 337-341

[5] J. Lusakowski *et al.*, "Ballistic and pocket limitations of mobility in nanometer Si metal-oxide semiconductor field-effect transistors", *Appl. Phys. Lett.*, vol. 87, pp. 053507-3, 2005.

[6] A. R. Brown , V. Huard, and A. Asenov "Statistical Simulation of Progressive NBTI Degradation in 45-nm technologiy pMOSFET ", *IEEE Trans. Electron Devices*, vol. 57, pp. 2320-2323, 2010.

[7] K. Huet, J. Saint-Martin, A. Bournel, S. Galdin-Retailleau, P. Dollfus, G. Ghibaudo, and M. Mouis, "Monte Carlo study of apparent mobility reduction in nano-MOSFETs", in *Proc. ESSDERC Conf.*, 2007, pp. 382-385.

[8] N. Seoane, A. Martinez, A. R. Brown J. R. Barker A. Asenov, "current variability in Si nanowire MOSFETs due to the random dopants in the source/Drain Regions: A fully 3-D NEGF simulation study", *IEEE Trans. Electron Devices*, vol. 56, pp. 1388-1395, 2009.

[9] J. Wang, E. Polizzi, A. Gosh, S. Datta, and M. Lundstrum, "Theoretical investigation of surface roughness scattering in silicon nanowire transistors", *Appl. Phys. Lett.*, vol. 87, p. 043101, 2005

[10] A. Svizhenko, P.W. Leu, and K. Cho, "Effect of growth orientation and surface roughness on electron transport in silicon nanowires", *Phys Rev. B*, vol. 75, p. 125417, 2007.

[11] M. Luisier, A. Schenk, and W. Fichtner, "Atomistic treatment of the interface roughness in Si nanowire transistors with different channel orientations", *Appl. Phys. Lett.*, vol. 90, p. 102103, 2007

[12] S. Jin, M.V. Fischetti, and T.-W. Tang, "Modeling of Surface-roughness scattering in Ultrathin-body SOI MOSFETs", *IEEE Trans. Electron Devices*, vol. 54, No 9, pp. 2191-2203, Sept. 2007.

[13] S. Poli, M. G. Pala, T. Poiroux, S. Deleonibus, and G. Baccarani, "Size dependence of surface-roughness-limited mobility in Silicon-nanowire FETs", *IEEE Trans. Electron Devices*, Vol. 55, No. 11, pp. 2968-2976, Nov. 2008.

[14] C. Buran *et al.*, "Three-Dimensional Real-Space Simulation of Surface Roughness in Silicon Nanowire FETs", *IEEE Trans. Electron Devices*, vol. 56, pp. 2186-2192 , Oct. 2009.

[15] A. Martinez *et al.*, "A study of the effect of the interface roughness on a DG-MOSFET using a full 2D NEGF technique", in *IEDM Tech. Dig.*, 2005, pp. 616-619.

[16] S.G. Kim *et al.*, "Full Three-Dimensional Quantum Transport Simulation of Atomistic Interface Roughness in Silicon Nanowire FETs", *IEEE Trans. Electron Devices*, vol. 58, pp. 1371-1380, May 2011.

[17] D. Esseni and A. Abramo, "Modeling of electron mobility degradation by remote Coulomb scattering in ultrathin oxide MOSFETs", *IEEE Trans. Electron Devices*, vol. 50, pp. 1665-1674, 2003.

[18] S. Saito, K. Torii, Y. Shimamoto, O. Tonomura, D. Hisamoto, et al., "Remote Charge Scattering limited mobility in field-effect transistors with $Si0_2$ and $Al_2O_3/Si0_2$ gate stacks", *J. Appl. Phys.*, vol. 98, pp. 113706, 2005.

[19] S. Barraud, L. Thevenod, M. Cassé, O. Bonno, and M. Mouis, "Modeling of Remote Coulomb scattering limited mobility in MOSFET with HfO_2/SiO_2 gate stacks", *Microelec. Eng.*, vol. 84, pp. 2404-2407, 2007.

[20] S. Poli, M.G. Pala and T. Poiroux, "Full Quantum Treatment of Remote Coulomb Scattering in Silicon Nanowire FETs" *IEEE Trans. Electron Devices*, vol. 56, pp. 1191-1198, June 2009.

[21] T. B. Tang, A.F Murray, and S. Roy "Methodology of statistical RTS noise analysis with charge-carrier trapping models", *IEEE Trans. Electron Devices*, vol. 57, pp. 1062-1070, 2009.

[22] M. Luisier, A. Schenk, and W. Fichtner, "Quantum transport in two- and three-dimensional nanoscale transistors: Coupled mode effects in the nonequilibrium Green's function formalism", *J. Appl. Phys.*, vol. 100, pp. 043713, 2006

[23] O. Roux Dit Buisson, G. Ghibaudo, and J. Brini, "Model for drain current RTS amplitude in small-area MOS transistors,", *Solid-State Electron.*, vol. 35, pp. 1273-1276, 1992.